

Photoemission Spectra of C_{60}^- ; Electron-phonon coupling, Jahn-Teller Effect and Superconductivity in the Fullerides

O. Gunnarsson

Max-Planck-Institut für Festkörperforschung, D-70506 Stuttgart, Germany

H. Handschuh, P.S. Bechthold, B. Kessler, G. Ganteför, and W. Eberhardt

Forschungszentrum Jülich GmbH, Institut für Festkörperforschung, D-52425 Jülich, Germany

(September 24, 1996)

A high-resolution experimental photoemission spectrum of C_{60}^- is compared with calculations including the Jahn-Teller effect and multiple phonon satellites. The spectra show discrete loss features due to the excitation of phonons. From the intensity of these features, electron-phonon coupling constants are derived, which support the electron-phonon mechanism for superconductivity. The systematic deviations from previously calculated coupling constants are discussed in detail.

Alkali doped fullerides A_3C_{60} ($A=K, Rb$) are, after the high T_c compounds, superconductors with some of the highest transition temperatures T_c known so far. Although the mechanism for the superconductivity in A_3C_{60} is not universally agreed upon, it is often argued that it is a “conventional” electron-phonon mechanism.¹⁻⁵ To establish the mechanism and to describe the properties within an electron-phonon model, it is crucial to obtain the electron-phonon coupling constants. This coupling is also important for other transport properties and the electronic structure in general.

There have been many calculations of this coupling,^{1,2,4,6} but the deviations between different calculations are large. Previous experimental estimates are based on the broadening of the phonons in doped compounds due to the decay of a phonon in an electron-hole pair⁷ observed in Raman⁸ and neutron scattering.⁹ The high energy modes exhibit, however, a large broadening, and it has not been possible to estimate their widths from these experiments. It is also unclear how the relation between the broadening and the coupling would be modified if corrections to Migdal’s theorem and the Jahn-Teller effect were included.

The fullerites and fullerides are formed by weakly interacting C_{60} molecules. From previous photoemission and inverse photoemission studies as well as from theory, it is known that the electronic states of the molecule are only slightly modified in the solid. The intramolecular phonons, believed to drive the superconductivity, are also only slightly changed in the solid. In fullerides each alkali atom dopes one electron into the LUMO of C_{60} . Thus the electron-phonon coupling observed in photoemission from gas phase negatively charged C_{60}^- can serve to determine the coupling constants for the superconductivity in A_3C_{60} .

Here we present a measured high resolution photoemission spectrum from the t_{1u} (LUMO) level of C_{60}^- . We

compare to a calculated spectrum using the sudden approximation, but including multiple phonon excitations (corrections to Migdal’s theorem) and the Jahn-Teller effect. Both effects are found to be crucial for the calculated spectra. By adjusting the electron-phonon coupling constants until the theoretical and experimental spectra agree, we can deduce values for the coupling constants. Photoemission from C_{60}^- has been studied earlier,¹⁰ but the resolution was not sufficient to allow an analysis of the type presented below.

The experimental setup¹¹ consists of a modified laser vaporization source, a time-of-flight mass spectrometer, an Excimer laser for electron detachment and a time-of-flight electron spectrometer. The clusters are produced by laser vaporization of graphite and successive cooling in a drift tube and a supersonic He expansion. This method generates various isomers of carbon clusters.¹² A dramatic change of the mass distribution enhancing the relative intensities of the fullerenes C_{44}^- , C_{50}^- , C_{60}^- , and C_{70}^- by two orders of magnitude is achieved by an annealing process right after the vaporization.¹³ This annealing is realized by a pulsed electric arc which is ignited within the Carbon-cluster and He-gas mixture. The clusters are then cooled in a long extender and the subsequent supersonic expansion. The negatively charged clusters are mass separated by a Wiley-McLaren TOF mass spectrometer. A bunch of cluster anions of a certain mass is irradiated by a UV-laser pulse (XeCl, 4.025eV). The kinetic energy of the detached electrons is measured using a “magnetic-bottle” type time-of-flight electron spectrometer.¹⁴ The energy resolution of the electron spectrometer is about 40 meV. The energy scale is calibrated using the data of the electron affinities of C_5^- , C_7^- and C_9^- .¹⁵

The inset of Fig. 1 shows the measured photoelectron spectrum of C_{60}^- . The intensity distribution has four main features between binding energies (BE) of 2.6 and 2.9 eV, a minimum at about 3 eV BE and a slowly increasing background signal beyond 3.1 eV BE. This photoelectron spectrum is observed only when the clusters are carefully annealed and cooled down properly. The feature located at 2.70 ± 0.05 eV BE is assigned to the transition from the electronic ground state of C_{60}^- into the electronic ground state of C_{60} . The additional features at higher BE correspond to energy loss processes due to electron-phonon coupling. An interpretation of the broad

feature between 3.1 eV and 3.4 eV BE is still uncertain. Since it is located in the fundamental gap region it cannot be attributed to an electronic excitation. It could be due to thermionic emission and/or the presence of a different isomer.

In C_{60}^{-1} the three-fold degenerate t_{1u} is singly occupied. Other orbitals are well separated from the t_{1u} orbital on the energy scale considered here and are therefore neglected. Due to the symmetry, the t_{1u} orbital can only couple to phonons (vibrations) with A_g or H_g symmetry. The degeneracy of the t_{1u} orbital is split under the distortion of H_g phonons, and this Jahn-Teller effect is essential for the results. We consider a model with a linear coupling to harmonic phonons

$$H = \varepsilon_0 \sum_{m=1}^3 \psi_m^\dagger \psi_m + \sum_{\nu=1}^{42} \omega_\nu b_\nu^\dagger b_\nu + \sum_{m=1}^3 \sum_{n=1}^3 \sum_{\nu=1}^{42} c_{nm}^\nu \psi_m^\dagger \psi_n (b_\nu + b_\nu^\dagger), \quad (1)$$

where the first term describes the electron, the second term the phonons and the third term the electron-phonon interaction. ψ_m^\dagger creates an electron in one of the three t_{1u} states, b_ν^\dagger creates a phonon in one of the 42 phonon modes (eight five-fold degenerate H_g phonons or 2 nondegenerate A_g phonons) and c_{nm}^ν is the coupling constant for the scattering of an electron from state n to state m under the creation or annihilation of a phonon of type ν . The form of the constants c_{nm}^ν for the five degenerate H_g modes is determined by symmetry,¹⁶ and there is therefore just one unknown parameter for each of the eight H_g modes and for the two A_g modes describing the absolute strength of the coupling. The relation of these coupling constants to the coupling λ_ν entering in superconductivity is given in the literature.¹⁶ The phonon frequencies were obtained from experiment.¹⁷

The vibration temperature T is of the order 200K, which is substantially lower than the energy of the lowest phonon mode ~ 400 K. We therefore assume that $T = 0$ and consider the ground-state wave function,

$$|\Phi\rangle = \left[\sum_{m=1}^3 a_m \psi_m^\dagger + \sum_{m=1}^3 \sum_{\nu=1}^{42} a_{m,\nu} \psi_m^\dagger b_\nu^\dagger + \sum_{m=1}^3 \sum_{\mu=1}^{42} \sum_{\nu=1}^{\mu} a_{m,\mu,\nu} \psi_m^\dagger b_\mu^\dagger b_\nu^\dagger + \dots \right] |vac\rangle, \quad (2)$$

where the first term describes a state with no phonon, the second term a state with one phonon and so on. We have considered states with up to five phonons. The Hamiltonian matrix corresponding to these basis states is calculated. The lowest eigenvalue and the corresponding eigenvector are calculated using Lanczos method.

We use the sudden approximation,¹⁸ where the emitted electron is assumed not to interact with the system left behind. It is further assumed that the energy dependence of the dipole matrix element to the final state can

be neglected.¹⁸ For the low photon energies considered here, the accuracy of these standard approximations is not clear. However, spectra measured with lower energy resolution at different photon energies ranging from 3.5 to 6.4eV show the same general shape of the photoemission features and therefore support the above assumptions. We take the spectrum shown in Fig. 1 which is accumulated with the best energy resolution and statistics as representative for this photon energy range.

For the final state of the neutral C_{60} molecule, there is no coupling between states with different number of phonons, since the electron has been emitted, and the eigenstates are therefore trivial. The photoemission spectrum is then expressed in terms of the coefficients in Eq. (2). A Gaussian broadening with the width (FWHM) 41 meV is introduced to take into account the experimental resolution.

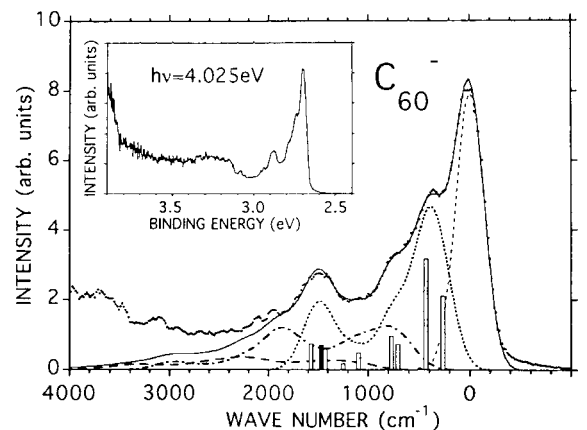


FIG. 1. The experimental (dots) and theoretical (full line) photoemission spectrum of C_{60}^{-} . The theoretical no loss (dashed), single loss (dotted), double loss (dashed-dotted) and triple loss (long-dashed) curves are also shown. The contributions of the different modes to the single loss curve are given by bars (H_g : open, A_g : solid). The inset shows the experimental spectrum over a larger energy range.

TABLE I. The partial electron-phonon coupling constants $\lambda_\nu/N(0)$ [in eV] according to the present estimates (PES) and according to the calculations by Antropov et al (Antrop)⁴ by Varma et al,¹ by Schluter et al² and by Faulhaber et al (Faul),⁶ as well as estimates based on neutron scattering (Neut).⁹ We also show the experimental energies (in cm^{-1}) of the modes. Σ shows the sum of the couplings to all the modes.

Mode	Energy	$\lambda_\nu/N(0)$					
		PES	Antrop	Varma	Schluter	Faul	Neut
$H_g(8)$	1575	.023	.022	.011	.009	.009	
$H_g(7)$	1428	.017	.020	.034	.013	.015	
$H_g(6)$	1250	.005	.008	.000	.003	.002	
$H_g(5)$	1099	.012	.003	.006	.001	.002	
$H_g(4)$	774	.018	.003	.000	.007	.010	.005
$H_g(3)$	710	.013	.003	.001	.004	.001	.001
$H_g(2)$	437	.040	.006	.001	.007	.010	.024
$H_g(1)$	271	.019	.003	.003	.008	.001	.014
$A_g(2)$	1470	.011	.011		.005		
$A_g(1)$	496	.000	.000		.000		
ΣH_g		.147	.068	.056	.052	.049	

In Fig. 1 we compare the experimental and theoretical spectra. The structures at about 400, 750 and 1500 cm^{-1} are mainly due to single phonon losses. There is, however, also a substantial contribution from double losses and triple losses as shown in Fig. 1. Therefore it is essential to include multiple phonon excitations, in particular since the higher order processes also influence the lower order ones. Although the theoretical spectrum depends rather sensitively on the coupling to the individual phonons, we cannot unambiguously determine the relative coupling to phonons close in energy, like $H_g(7)$, $H_g(8)$ and $A_g(2)$. The coupling constants used in Fig. 1 are shown in Table I. The couplings to the $A_g(1)$ and $A_g(2)$ modes are chosen to agree with calculated values.⁴ The coupling to $A_g(2)$ can, however, be varied between $\lambda_{10}/N(0)=0.00$ and 0.03 without essentially worsening the fit, if the total coupling to $H_g(7)$ and $H_g(8)$ is changed correspondingly (between 0.07 and 0.00). Zero coupling to the $H_g(7)$ and $H_g(8)$ modes is, however, inconsistent with the belief that a large broadening by the electron-phonon coupling is the reason these modes have not been observed in the doped compounds in neutron scattering. The coupling to $A_g(1)$ can also be increased a bit without worsening the fit, if the couplings to the $H_g(1)$ and $H_g(2)$ modes are reduced. There is some additional experimental weight above the main peak, which could be due to energy gain processes, where the electron picks up energy from a thermally excited phonon in the initial state.

The contribution of the H_g phonons to the total energy differs strongly in the weak- or strong-coupling regimes.¹⁹ Defining

$$E_{JT} = \frac{2}{15} \sum_{\nu=1}^{40} \sum_{i=1}^3 \sum_{j=1}^3 \frac{|c_{nm}^\nu|^2}{\omega_\nu}, \quad (3)$$

the H_g contribution to the total energy is $E_{H_g} = -\frac{5}{2}E_{JT}$ in the weak-coupling limit, but only only $E_{H_g} = -E_{JT}$ in the strong-coupling limit. In contrast, defining E_s for the A_g phonons in a similar way, the A_g contribution to the total energy is $E_{A_g} = -\frac{5}{2}E_s$, independently of the coupling strength. We introduce the center of gravity, $E_{c.g.}$ of the spectrum relative to the no-loss peak. For the model considered here, $E_{c.g.} = E_{H_g} + E_{A_g}$ in the weak- and strong-coupling limits, but $|E_{c.g.}| < |E_{H_g} + E_{A_g}|$ for intermediate couplings. With the parameters in Table I, we find that $E_{H_g} + E_{A_g} \approx -1.7(E_{JT} + E_s)$ and $E_{c.g.} \approx -(E_{JT} + E_s)$, i.e., C_{60} is in the intermediate- to strong-coupling regime. In the weak-coupling limit, we could neglect the Jahn-Teller effect by using couplings c_{nm}^ν appropriate for A_g modes and by choosing the absolute strength so that the spectra nevertheless agree. Since C_{60}^- is not in the weak-coupling limit, we would then, however, deduce a $|E_{c.g.}|$ which is larger by a factor 2.5 and need to reduce the couplings correspondingly to reproduce the experimental spectrum. It is therefore crucial to take the Jahn-Teller effect into account.

In Table I we compare the deduced coupling constants with various calculations. The total λ contains only the H_g contributions, since the A_g contributions should be largely screened out in the solid.¹⁶ The new λ is a factor 2-3 larger than the calculated values. Although the different calculations give quite different distributions of couplings to different modes, they all find the strongest coupling to one of the high-lying modes, while the present analysis gives the strongest coupling to the second lowest mode. The calculated couplings are extremely sensitive to the phonon eigenvectors.⁴ If, for instance, the correct 2nd and 8th eigenvectors are $e_2 = \sqrt{0.95}e_2^A + \sqrt{0.05}e_8^A$ and $e_8 = -\sqrt{0.05}e_2^A + \sqrt{0.95}e_8^A$, where e_2^A and e_8^A are the eigenvectors of Antropov et al,⁴ the corresponding couplings would become $\lambda_2/N(0) = 0.033$ eV and $\lambda_8/N(0) = 0.019$ eV (instead of 0.006 and 0.022 eV) and the sum of these couplings would almost double from 0.028 to 0.052 eV. It is an interesting issue if the discrepancies in Table I can be explained by such errors in the eigenvectors or if there are more fundamental problems.

Table I also compares the present couplings with the couplings deduced from inelastic neutron scattering,⁹ using⁷

$$\frac{\lambda_\nu}{N(0)} = \frac{\gamma_\nu g_\nu}{2\pi\omega_\nu^2 N(0)^2}, \quad (4)$$

where γ_ν is the line width of a phonon loss peak, g_ν is the degeneracy of the phonon, ω_ν is its frequency and $N(0)$ is the density of states determined from NMR.²⁰ Eq. (4) is based on Migdal's theorem and neglects Jahn-Teller effects. The experience above suggests that the coupling constants derived from Eq. (4) may therefore be too small. For the two lowest modes, with the strongest coupling, Eq. (4) gives a coupling that is a factor 1.5 smaller than the present coupling but a factor 2.5-10 larger than the calculated ones.

Finally, we consider the implications for superconductivity. We treat A_3C_{60} , and describe the t_{1u} band by a 0.5 eV broad band with $N(0)=7.2$ (A=K) and 8.1 (A=Rb) states per spin and eV.²⁰ The repulsive Coulomb interaction is described by a pseudopotential μ^* . We have solved the Eliashberg equation, using the couplings deduced here. To reproduce the T_c (18 K) of K_3C_{60} and (28 K) of Rb_3C_{60} , we have to use $\mu^* = 0.6$. This is even somewhat larger than the fairly large value 0.4, obtained in earlier calculations.⁵ Although the calculations of μ^* and T_c involve many approximations, they illustrate that even if retardation effects may not reduce μ^* for A_3C_{60} nearly as much as is assumed for conventional superconductors,⁵ λ may still be large enough to explain T_c in terms of an electron-phonon mechanism. We have calculated the isotope effect and found $\alpha = 0.32$ for K_3C_{60} and $\alpha = 0.37$ for Rb_3C_{60} . There are several measurements of the isotope effect for Rb_3C_{60} ,²¹⁻²⁴ giving very different results. The probably most reliable measurement, using 99 % substitution, gave $\alpha = 0.30 \pm 0.05$.²⁴ We have further calculated the reduced gap $2\Delta/T_c$ and found 3.59 for K_3C_{60} and 3.66 for Rb_3C_{60} . Such BCS-like (3.52) values are also found in optical experiments²⁵ (3.44 and 3.45 for K_3C_{60} and Rb_3C_{60} , respectively) and in muon spin relaxation experiments²⁶ (3.6 for Rb_3C_{60}), while tunneling experiments give a much larger result²⁷ (5.3 for Rb_3C_{60}).

We have presented experimental and theoretical photoemission spectra for C_{60}^- , and deduced electron-phonon coupling constants. The proper inclusion of the Jahn-Teller effect and multiple phonon excitations in the calculations was found to be essential. It would be very interesting to go beyond the sudden approximation used here. The deduced couplings are consistent with inelastic neutron scattering data, but a factor 2-3 larger than available calculations. This raises interesting questions about the accuracy of the calculational methods, e.g., for the phonon eigenvectors. The deduced couplings together with an earlier estimate of the Coulomb pseudopotential μ^* , give T_c of the correct order of magnitude, providing support for electron-phonon coupling being the driving mechanism for the superconductivity.

We want to thank P. Bruhwiler for helpful discussions.

¹ C.M. Varma, J. Zaanen, and K. Raghavachari, *Science* **254**, 989 (1991).

² M. Schluter, M. Lanno, M. Needles, G.A. Baraff, and D. Tomanek, *Phys. Rev. Lett.* **68**, 526 (1992); *J. Phys. Chem. Solids* **53**, 1473 (1992).

³ I.I. Mazin, S.N. Rashkeev, V.P. Antropov, O. Jepsen, A.I. Liechtenstein, and O.K. Andersen, *Phys. Rev. B* **45**, 5114 (1992).

⁴ V.P. Antropov, O. Gunnarsson and A.I. Liechtenstein, *Phys. Rev. B* **48**, 7551 (1993).

⁵ O. Gunnarsson and G. Zwicknagl, *Phys. Rev. Lett.* **69**, 957 (1992). O. Gunnarsson, D. Rainer, and G. Zwicknagl, *Int. J. Mod. Phys. B* **6**, 3993 (1992).

⁶ J.C.R. Faulhaber, D.Y.K. Ko, and P.R. Briddon, *Phys. Rev. B* **48**, 661 (1993).

⁷ P.B. Allen, *Phys. Solid State Commun.* **14**, 937 (1974).

⁸ M.G. Mitch, S.J. Chase, and J. S. Lannin, *Phys. Rev. Lett.* **68**, 883 (1992); *Phys. Rev. B* **46**, 3696 (1992).

⁹ K. Prassides, C. Christides, M.J. Rosseinsky, J. Tomkinson, D.W. Murphy, and R.C. Haddon, *Europhys. Lett.* **19**, 629 (1992); K. Prassides, J. Tomkinson, C. Christides, M.J. Rosseinsky, D.W. Murphy, and R.C. Haddon, *Nature* **354**, 462 (1991).

¹⁰ L.-S. Wang, O. Cheshnovsky, R.E. Smalley, J.P. Carpenter, and S.J. Hwu, *J. Chem. Phys.* **96**, 4028 (1992).

¹¹ C-Y. Cha, G. Ganteför, W. Eberhardt, *Rev.Sci.Instrum.* **63**, 5661 (1992).

¹² G.v. Helden, M-T. Hsu, P.R. Kemper, M.T. Bowers, *J.Chem.Phys.* **95**, 3835 (1991).

¹³ H. Handschuh, G. Ganteför, B. Kessler, P.S. Bechthold, W. Eberhardt, submitted to *Phys. Rev. Lett.*

¹⁴ P. Kruit, F.H. Read, *J.Phys.* **E16**, 313 (1983).

¹⁵ D.W. Arnold, S.E. Bradforth, T.N. Kitsopoulos, D.M. Neumarck, *J.Chem.Phys.* **95**, 8753 (1991).

¹⁶ M. Lannoo, G.A. Baraff, M. Schlüter, and D. Tomanek, *Phys. Rev. B* **44**, 12106 (1991).

¹⁷ D.S. Bethune, G. Meijer, W.C. Tang, H.J. Rosen, W.G. Golden, H. Seki, C.A. Brown, and M.S. de Vries, *Chem. Phys. Lett.* **179**, 181 (1991).

¹⁸ L. Hedin and S. Lundqvist, *Solid State Physics Vol. 23* (eds. H. Ehrenreich, D. Turnbull and F. Seitz, Academic, New York) p. 1.

¹⁹ A. Auerbach, N. Manini and E. Tosatti, *Phys. Rev. B* **49**, 12998 (1994); N. Manini, E. Tosatti and A. Auerbach, *ibid* **49**, 13008 (1994); A. Auerbach, *Phys. Rev. Lett.* **72**, 2931 (1994).

²⁰ V.P. Antropov, I.I. Mazin, O.K. Andersen, A.I. Liechtenstein, and O. Jepsen, *Phys. Rev. B* **47**, 12373 (1993).

²¹ A.P. Ramirez, A.R. Kortan, M.J. Rosseinsky, S.J. Doclos, A.M. Muzsca, R.C. Haddon, D.W. Murphy, A.V. Makhija, S.M. Zahurak, and K.B. Lyons, *Phys. Rev. Lett.* **68**, 1058 (1992).

²² T.W. Ebbesen, J.S. Tsai, K. Tanigaki, J. Tabuchi, Y. Shimakawa, Y. Kubo, I. Hirose, and J. Mizuki, *Nature* **355**, 620 (1992).

²³ A.A. Zakhidov, K. Imaeda, D.M. Petty, K. Yakushi, H. Inokuchi, K. Kikuchi, I. Ikemoto, S. Suzuki, and Y. Achiba, *Phys. Lett. A* **164**, 355 (1992).

²⁴ C.C. Chen and C.M. Lieber, *Science* **259**, 655 (1993).

²⁵ L. Degiorgi, G. Briceno, M.S. Fuhrer, A. Zettl, and P. Wachter, *Nature* **369**, 541 (1994).

²⁶ R.F. Kiefl, W.A. MacFarlane, K.H. Chow, S. Dunsiger, T.L. Duty, T.M.S. Johnston, J.W. Schneider, J. Sonier, L. Brard, R.M. Strongin, J.E. Fischer, and A.B. Smith III, *Phys. Rev. Lett.* **25**, 3987 (1993).

²⁷ Z. Zhang, C.-C. Chen, S.P. Kelty, H. Dai, and C.M. Lieber, *Nature* **353**, 333 (1991).